# Minimal model for kinetic arrest

P. Pal,[1,*] C. S. O'Hern,[1,†] J. Blawzdziewicz,[1,†] E. R. Dufresne,[1,‡] and R. Stinchcombe[2]

[1]*Department of Mechanical Engineering, Yale University, New Haven, Connecticut 06520-8286, USA*
[2]*Rudolf Peierls Centre for Theoretical Physics, University of Oxford, 1 Keble Road, Oxford, OX1 3NP, United Kingdom*

To elucidate slow dynamics in glassy materials, we introduce the figure-8 model in which $N$ hard blocks undergo Brownian motion around a circuit in the shape of a figure 8. This system undergoes kinetic arrest at a critical packing fraction $\phi = \phi_g < 1$, and for $\phi \approx \phi_g$ long-time diffusion is controlled by rare, cooperative, "junction-crossing" particle rearrangements. We find that the average time between junction crossings $\tau_{JC}$, and hence the structural relaxation time, does not simply scale with the configurational volume $\Omega_c$ of transition states, because $\tau_{JC}$ also depends on the time to complete a junction crossing. The importance of these results in understanding cage-breaking dynamics in glassy systems is discussed.

## I. INTRODUCTION

Glass transitions occur in myriad systems that span a wide range of length scales [1] including atomic, polymeric, and colloidal systems. When cooled or compressed sufficiently fast, glass-forming materials undergo a transition from an ergodic liquid state to an amorphous solidlike glassy state [2–4]. Glassy dynamics is characterized by several common features [5]. For example, the viscosity and structural relaxation times diverge super-Arrheniusly near the glass transition, and the long-time self-diffusion constant becomes extremely small. Correspondingly, a plateau develops in the particle mean-square displacement (MSD). As the system approaches the glass transition, the plateau extends to longer and longer times [6–8], signaling kinetic arrest associated with the formation of cages of neighbors around each particle. Structural relaxation occurs through a series of rare cage-breaking events, in which particles in the nearest-neighbor and further shells move cooperatively so that caged particles can escape [4].

The last feature is emphasized in Fig. 1, where we show results from simulations of a 50-50 bidisperse mixture of hard disks with diameter ratio 1.4 in the supercooled liquid regime. In Fig. 1(a), we plot displacements of a focus particle as it moves between three cages $\alpha$, $\beta$, and $\gamma$. In Figs. 1(b)–1(f), we monitor the focus particle and its neighbors as it breaks out of cage $\alpha$ and becomes trapped in $\beta$. Two processes are required for cage breaking to occur. First, an opening must appear in the shell of nearest neighbors [cf. Figs. 1(c) and 1(d)] and, second, particles beyond the nearest-neighbor shell must make sufficient room for the escaping particle [cf. Figs. 1(d) and 1(e)]. If the material beyond the nearest-neighbor shell behaves as a fluid, the second process occurs easily, and the first is the rate-controlling step. How-

ever, at higher packing fractions $\phi$ structural relaxation outside the nearest-neighbor shell relies on other cage rearrangements. Near the glass transition, particles cannot escape from their cages because surrounding particles are trapped in their own cages and unable to make room. Geometrically, this is similar to the mechanism behind rush-hour traffic jams, where cars cannot exit an intersection because there is not enough room in the street in front of them. This, in turn, prevents cars in the perpendicular direction from entering the intersection, which causes a cascade of delays, leading to a city-wide traffic jam.

To elucidate geometrical mechanisms responsible for slow dynamics in glassy materials, we introduce a "minimal" figure-8 model that captures fundamental aspects of caging
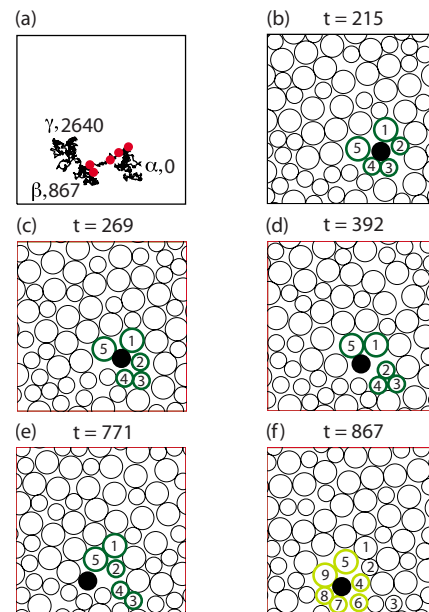


FIG. 1. (Color online) (a) Trajectory taken from molecular dynamics simulations of 64 bidisperse hard disks over a period in which the focus particle explores three cages $\alpha$, $\beta$, and $\gamma$. The cage-entrance times are provided. The shaded circles correspond to snapshots in (b)–(f), which are labeled by time $t$. The filled disk corresponds to the focus particle in (a) and particles forming the $\alpha$ and $\beta$ cages are outlined in dark green (dark gray) and light green (light gray), respectively.

*Also at Department of Applied Physics, Yale University, New Haven, CT 062520, USA.

†Also at Department of Physics, Yale University, New Haven, CT 062520, USA.

‡Also at Department of Physics and Department of Chemical Engineering, University of Oxford, Oxford, OX1 3NP, United Kingdom
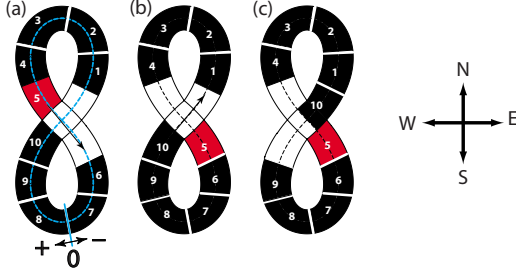
FIG. 2. (Color online) Schematic of the figure-8 model near $\phi_g$. (a)–(c) depict a junction-crossing event. Initially half of the particles are in each lobe. Between (a) and (b) particle 5 crosses the junction. Between (b) and (c) particle 10 moves into the junction in the direction of the arrow. In (c) the center of particle 10 resides in the upper lobe, which completes the junction-crossing event.

and cooperative motion. As illustrated in Fig. 2, in our model $N$ hard blocks undergo single-file diffusion around a continuous course in the shape of a figure 8. Kinetic arrest at large $\phi$ occurs because particles moving in one direction must vacate the junction to allow those moving in the perpendicular direction to pass through the junction. This model has several appealing features. First, it is one of the simplest continuum models that captures kinetic arrest. Second, to mimic a glassy material, the figure 8 model can be generalized to the "Manhattan" model, which includes an arbitrary number of intersections and particles per lobe. Third, experimental realizations of this model can be performed, for example, by confining colloidal suspensions in narrow channels [9,10]. Also, the figure 8 model may provide insights into unanswered questions concerning glassy systems: (1) What mechanisms give rise to cage-breaking events and how are they related to dynamical heterogeneities [11,12]? (2) Why does significant slowing down occur in dense particulate systems below random close packing? (3) What is the form of the divergence of the structural relaxation time near the glass transition?

## II. FIGURE-8 MODEL

We now provide a detailed description of the figure-8 model. The upper and lower lobes of a channel of length $L$ intersect at a square junction with unit dimensions. The particles (hard blocks with length $l=1$) undergo single-file Brownian diffusion, implemented numerically using Monte Carlo single-particle moves chosen from a Gaussian distribution. The contour length and average gap $\Delta$ per particle satisfy the relation $\phi = N/L = 1/(1+\Delta)$. The particles are not allowed to turn at the intersection. Therefore, particles move through the junction in one of two possible modes: (1) from northwest to southeast and vice versa or (2) from northeast to southwest and vice versa. To switch modes, particles moving in one mode must vacate the junction to allow particles in the other to enter the junction. We focus our analysis on small systems with $2 \leq N \leq 20$ particles to imitate cooperative cage rearrangements in finite-size local regions in glass-forming liquids (such as those depicted in Fig. 1).

## III. NUMERICAL RESULTS

The dynamics is monitored by measuring the mean square displacement of the blocks, $\Sigma(\tau) = \sum_{i=1}^{N} \langle [x_i(\tau) - x_i(0)]^2 \rangle / N$,
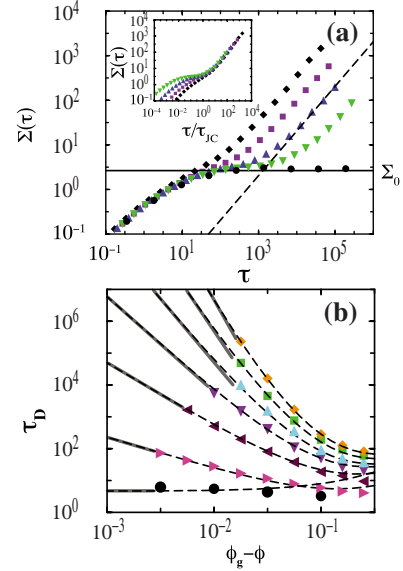


FIG. 3. (Color online) (a) MSD $\Sigma(\tau)$ normalized by $\Delta^2$ for $N=10$ at $\phi_g - \phi = 0.1$ (diamonds), 0.056 (squares), 0.032 (upward triangles), 0.018 (downward triangles), and $10^{-5}$ (circles). The time $\tau$ is normalized by $\Delta^2/2D_s$, where $D_s$ is the short-time diffusion constant. The dashed line is a fit to $\Sigma(\tau) = 2D\tau$ for large $\tau$ at $\phi_g - \phi = 0.032$. The inset shows the same data versus time normalized by the average junction-crossing time $\tau_{JC}$. (b) Diffusion time $\tau_D$ vs $\phi_g - \phi$ for $N=2,4,6,8,10,12,14$ (from below). Fits to Eq. (9) (dashed lines) with $\alpha(N)$ as a free parameter and the asymptotic behavior (1) (solid lines) are also shown. $\alpha(N)$ was chosen to match the smallest $\phi_g - \phi$ data points for each $N$.

where $x_i(\tau)$ is the position of the center of block $i$ at time $\tau$. From numerical results in Fig. 3(a), for sufficiently large $\phi$ the MSD develops a plateau $\Sigma = \Sigma_0$, which signals the onset of slow dynamics. The length of the plateau increases as $\phi$ approaches a critical value $\phi_g$. However, for any $\phi < \phi_g$, the MSD finally becomes diffusive, with $\Sigma(\tau) = 2D\tau$ as $\tau \to \infty$. This behavior mimics slow dynamics in glassy materials. The time $\tau_D = \Sigma_0/2D$ for the system to reach the long-time diffusive regime is plotted in Fig. 3(b) as a function of $\phi$ for several system sizes $N$. As indicated by the solid lines, for $\phi \to \phi_g$, $\tau_D$ exhibits a power-law divergence

$$\tau_D^{-1} \sim (\phi_g - \phi)^{N/2-1}. \quad (1)$$

To gain insight into the system dynamics near $\phi_g$ and explain the critical behavior (1), we consider sample trajectories depicted in Fig. 4. We see that most often particles are evenly divided between the two lobes, and the junction is occupied by one or two particles in the same mode. Occasionally, the junction becomes unoccupied and the direction of motion changes. However, an analysis of the trajectories shows that not all such switches produce significant particle displacements. On rare occasions, a switch of the direction of motion results in a significant shift of all particles. Such a junction-crossing rearrangement requires that a specific sequence of events unfolds as shown schematically in Fig. 2 and in actual trajectories in Fig. 4. First, a given particle completely crosses the intersection and enters a lobe that
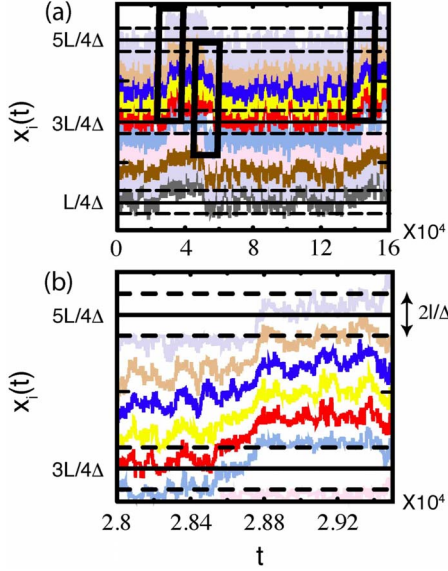
FIG. 4. (Color online) (a) Trajectories $x_i(t)$ scaled by $\Delta$ for each particle $i$ over a period during which three junction-crossing events (highlighted in black rectangles) occur. The solid horizontal lines correspond to the center of the junction at $x = (L/4, 3L/4, 5L/4, \ldots)$, and the long-dashed horizontal lines are displaced by $l$ from them. (b) Closeup of trajectories during the first junction-crossing event. Online each particle trajectory corresponds to a distinct color, while in print only neighboring particle trajectories have distinct gray scales.

already has $N/2$ particles, thus creating a compressed lobe with $N/2+1$ particles. Next, another particle leaves the compressed lobe from the other end (which requires that the intersection is free) and enters the uncompressed lobe, so that the particles are again evenly distributed between the two lobes. Three such junction-crossing events are highlighted in Fig. 4(a), and a closeup of one of them is shown in Fig. 4(b).

From geometrical constraints, junction crossings can occur only when $N/2+1 \leq L/2-1$, which yields $\phi_g = N/(N+4)$. When $\phi \to \phi_g$, the available space in the compressed lobe tends to zero, giving rise to the slow dynamics and the plateau of the MSD in Fig. 3. In the inset to Fig. 3(a), we replot the MSD with $\tau$ scaled by the average time between junction-crossing rearrangements, $\tau_{\mathrm{JC}}$. The rescaled MSD for different $\phi$ collapse at long times, which confirms that long-time diffusion is controlled by junction-crossing events. An analysis of the system geometry indicates that a junction crossing event produces an average particle shift $\delta = \frac{3}{2} + \Delta - N^{-1}$ with $2D = \delta^2/\tau_{\mathrm{JC}}$.

## IV. THEORETICAL DESCRIPTION

Since the slow evolution for $\phi \to \phi_g$ results from an entropic bottleneck associated with the creation of a compressed lobe, we expect that the scaling behavior of $\tau_D \sim \tau_{\mathrm{JC}}$ with $\Delta\phi$ can be obtained by calculating the corresponding volume in configuration space. In equilibrium, the fraction of time $t_c/T$ the system spends in the compressed configuration is

$$\frac{t_c}{T} = \frac{\Omega_c \Omega_u}{\Omega}, \tag{2}$$

where $\Omega_{c,u}$ and $\Omega$ are configuration integrals for the compressed (uncompressed) lobe and whole system, respectively. $\Omega_{c,u}$ and $\Omega$ can be written in terms of the configurational integral $\omega(L_0, M) = (L_0 - M)^M/M!$ for a one-dimensional 1D gas of $M$ unit-length hard rods confined within length $L_0$ (Tonks gas [13]). The compressed and uncompressed lobes correspond to a Tonks gas of length $L_1 = L/2 - 1$ with $N_{c,u} = N/2 \pm 1$ particles. Accordingly we have

$$\Omega_c = \frac{\Delta_c^{N/2+1}}{(N/2+1)!}, \tag{3a}$$

$$\Omega_u = \frac{\Delta_u^{N/2-1}}{(N/2-1)!}, \tag{3b}$$

where $\Delta_c = \frac{1}{2}(L-N-4)$ and $\Delta_u = \frac{1}{2}(L-N)$ denote the free space in the compressed and uncompressed regions. The configurational integral for the whole system can be expressed as a combination of Tonks-gas results,

$$\Omega = 2\omega(L,N) - \sum_{\substack{N_1,N_2 \\ N_1+N_2=N}} \omega(L_1,N_1)\omega(L_1,N_2), \tag{4}$$

where the 2 corresponds to the two directions of motion for particles in the intersection and the subtracted sum prevents double counting of configurations with an empty intersection.

At $\phi_g$ the free space in the compressed lobe $\Delta_c$ vanishes, which is the source of the kinetic arrest. The structural relaxation time for $\phi \approx \phi_g$ is calculated using (2) to estimate the average time between junction crossings $\tau_{\mathrm{JC}} = T/n$ (where $n$ is the number of crossing events). Assuming that on average during a single junction-crossing event the system spends time $\tau_c = t_c/n$ with one compressed and one uncompressed lobe, we obtain

$$\tau_D^{-1} \sim \tau_{\mathrm{JC}}^{-1} = \frac{t_c}{T}\tau_c^{-1} = \frac{\Omega_c\Omega_u}{\Omega}\tau_c^{-1}, \tag{5}$$

which links the structural relaxation time to the ratio of the configurational integrals (3) and (4). Using (3a), free space in the compressed lobe can be written in terms of $\Delta\phi$,

$$\Omega_c \sim (\phi_g - \phi)^{N/2+1}. \tag{6}$$

Thus, one might expect that $\tau_D^{-1} \sim \Omega_c \sim (\phi_g - \phi)^{N/2+1}$, i.e., the inverse diffusion time scales with the number of transition configurations. (This assumption is frequently adopted in analyses of cooperative glassy dynamics [14].) However, our numerical results do not support this hypothesis, and instead we observe a weaker singularity (1).

The anomalous behavior (1) stems from the fact that not only $\Omega_c$ but also $\tau_c$ vanishes at $\phi_g$. This can be demonstrated by noting that Brownian dynamics of a 1D gas of hard rods can be mapped onto a 1D system of point particles with interparticle distances equal to the gaps $\Delta x_i = x_i - x_{i-1} - 1$ between rods in the original Tonks gas. Since a gas of point particles does not involve a characteristic length scale, the

entire stochastic process $(\Delta x_1(t), \ldots, \Delta x_M(t))$ for systems of different $\phi$ (but corresponding initial conditions) can be scaled onto each other by introducing rescaled variables

$$\Delta x_i(\tilde{t}) = \lambda^{-1} \Delta x_i(\lambda^{-2} t), \tag{7}$$

where $\lambda$ is an appropriate scaling factor (e.g., the average interparticle gap). In the above relations $\Delta x_1$ is the gap between the first particle and the position at which the boundary condition is applied; the boundary condition on the other end of the domain is given by $\Sigma_{i=1}^{M} \Delta x_i$.

To apply the scaling relation (7) to our system we recall that a junction-crossing event requires that particles are divided between the compressed and uncompressed lobes. Particles in the compressed lobe evolve as a 1D Tonks gas until an interaction occurs with a particle that initially resided in the uncompressed lobe. Evolution of particles in the compressed lobe can be rescaled exactly even if a particle leaves this lobe and enters the junction, because both the particle positions and boundary conditions can be rescaled. This is important because a particle on the border of the junction enters and leaves the compressed lobe multiple times before a junction-crossing event is completed.

The mapping (7) of the dynamics of the compressed lobe implies that the corresponding scaling will also hold for the average time $\tau_c$ that the system spends in the compressed configuration. Taking $\lambda = \Delta_c$, we find that

$$\tau_c^{-1} = \alpha \Delta_c^{-2}, \tag{8}$$

where $\alpha$ is a proportionality constant. Combining the above relation with (5) yields [15]

$$\tau_D^{-1} = \frac{\alpha \Delta_c^{-2} \Omega_c \Omega_u}{\Omega}, \tag{9}$$

which, according to Eqs. (6) and (8), agrees with the observed anomalous scaling (1). In Fig. 3(b), we show that Eq. (9) accurately represents the long-time diffusive dynamics not only when $\phi \to \phi_g$, but also at moderate $\phi$.

## V. CONCLUSIONS AND FUTURE DIRECTIONS

To summarize, we introduced the figure-8 model, which exhibits kinetic arrest when $\phi \to \phi_g$. We showed that for $\phi \approx \phi_g$ long-time diffusion is controlled by rare, cooperative, junction-crossing events, and we determined the configuration-space volume $\Omega_c$ corresponding to the transition states associated with junction crossings. We also demonstrated that the inverse structural relaxation time $\tau_D^{-1}$ does not scale with the volume $\Omega_c$ as $\phi \to \phi_g$, but the scaling also involves a singular factor associated with the accelerated evolution of compressed particle configurations in the volume $\Omega_c$. We predict that similar anomalous behavior may occur in glassy materials when a cage rearrangement requires compression of the material surrounding the cage.

There are several possible extensions of the figure-8 model that may shed light on important features of the glass transition (such as dynamic heterogeneities and aging phenomena [16,17]). We expect that these phenomena can be characterized by expanding the approach used here [18]. One generalization of the figure-8 model we are now pursuing involves increasing the number of junctions $j$ and determining how $\phi_g$ depends on $j$ and $N$ in a network of cross-linked channels. Similar to the figure-8 model, the multijunction system exhibits kinetic arrest at $\phi_g$ below close packing. An analysis of this class of models will shed light on mechanisms that give rise to slow dynamics in glass-forming materials.

[1] C. A. Angell, Science **267**, 1924 (1995).
[2] P. N. Pusey and W. van Megen, Nature (London) **320**, 340 (1986).
[3] A. van Blaaderen and P. Wiltzius, Science **270**, 1177 (1995).
[4] E. R. Weeks, J. C. Crocker, A. C. Levitt, A. Schofield, and D. A. Weitz, Science **287**, 627 (2000).
[5] P. G. Debenedetti and F. H. Stillinger, Nature (London) **410**, 259 (2001).
[6] B. Doliwa and A. Heuer, Phys. Rev. E **61**, 6898 (2000).
[7] D. Thirumalai and R. D. Mountain, Phys. Rev. E **47**, 479 (1993).
[8] H. Miyagawa, Y. Hiwatari, B. Bernu, and J. P. Hansen, J. Chem. Phys. **88**, 3879 (1988).
[9] C. Lutz, M. Kollmann, and C. Bechinger, Phys. Rev. Lett. **93**, 026001 (2004).
[10] B. Lin, M. Meron, B. Cui, S. A. Rice, and H. Diamant, Phys.

Rev. Lett. **94**, 216001 (2005).
[11] C. Donati, J. F. Douglas, W. Kob, S. J. Plimpton, P. H. Poole, and S. C. Glotzer, Phys. Rev. Lett. **80**, 2338 (1998).
[12] M. D. Ediger, Annu. Rev. Phys. Chem. **51**, 99 (2000).
[13] L. Tonks, Phys. Rev. **50**, 955 (1936).
[14] G. Adam and J. H. Gibbs, J. Chem. Phys. **43**, 139 (1965).
[15] In the large-$N$ limit, $\tau_D \sim \exp(1/\Delta\phi)$ for $\Delta\phi \to 0$, but this limit is not the focus of our study.
[16] G. C. Cianci, R. E. Courtland, and E. R. Weeks, Solid State Commun. **139**, 599 (2006).
[17] P. Wang, C. Song, and H. A. Makse, Nat. Phys. **2**, 526 (2006).
[18] R. Stinchcombe and M. Depken, Phys. Rev. Lett. **88**, 125701 (2002); M. Depken and R. Stinchcombe, Phys. Rev. E **71**, 065102 (2005); A. Lefévre, L. Berthier, and R. Stinchcombe, *ibid.* **72**, 010301(R) (2005).